

## Growth of Breath Figures

D. Beysens<sup>(a)</sup> and C. M. Knobler

*Department of Chemistry and Biochemistry, University of California, Los Angeles, California 90024*

(Received 14 July 1986)

Measurements are reported of the growth of breath figures, the patterns that form when a vapor is condensed onto a cold surface. The pattern for water on glass was studied by direct observation and light scattering as a function of the contact angle  $\theta$ , flux  $F$ , degree of supersaturation  $\Delta T$ , and time  $t$ . When  $\theta = 0^\circ$ , a uniform layer forms whose thickness grows as  $t$  at constant  $F$  and  $\Delta T$ . For  $\theta = 90^\circ$  droplets are formed; at constant  $F$  and  $\Delta T$  the radius of an isolated droplet grows as  $t^{0.23}$ , but as a result of coalescences the average droplet radius grows as  $t^{0.75}$ . The growth process is self-similar—coalescences simply rescale the distances and leave the basic droplet pattern unaltered.

PACS numbers: 68.10.Jy, 64.60.Qb, 82.60.Nh

Breath figures are the patterns formed when one breathes on a cold surface. Depending on the wetting properties of the surface, the condensed fluid can form either a uniform film, which appears dark, or an assembly of droplets, which scatters light and appears white. Breath figures have long been used<sup>1</sup> as a simple and effective tool to detect oil contamination on glass surfaces; even a monolayer of oil can be observed. Although a large body of literature exists on heterogeneous nucleation, there is surprisingly little known about the growth of fluid phases on surfaces, and we know of no quantitative studies of breath figures. The nucleation and growth of these condensation patterns is related to other problems of interest in the kinetics of phase transition and there is a connection as well to questions of wetting and surface roughness.<sup>2</sup> We have therefore begun detailed studies of the structure and the kinetics of growth of breath figures; this Letter describes our first results, which have some unexpected features.

The basic experimental procedure consists of streaming a gas saturated with a fluid across a glass plate that has been cooled. The resulting pattern that evolves is studied either by direct microscopic observation or by light scattering. The parameters that can be varied are the nature of the substrate (glass, sapphire, etc.), its temperature  $T_S$ , the temperature of the gas  $T_G$ , the gas flow rate  $F$ , and the percentage saturation  $w$ . The contact angle of the fluid on the substrate can also be altered by treatment of the surface.

This study is concerned only with the condensation of water vapor on a vertical surface. The carrier gas was nitrogen, which was filtered and then bubbled through distilled water. The gas flow was controlled by a needle valve and measured with a flow meter. The degree of saturation, which was always close to 100%, was monitored with a hygrometer. The gas temperature was typically 23 °C. At the start of an experiment, the flow conditions were established and then a bypass valve was closed to initiate the flow to the surface

through a glass nozzle 6 mm in diameter, whose tip was located 1 cm from the glass. The temperature of the glass could be controlled within the range  $-15$ – $70$  °C by a Peltier element coupled to a water thermostat; a thermocouple was used to measure the temperature, which was kept constant to  $\pm 0.2$  °C. During an experiment  $\Delta T = T_G - T_S$ ,  $w$ , and  $F$  were held constant; hence the measurements were always carried out at constant supersaturation. On very humid days the condensation of water from the atmosphere affected the measurements. The slide was therefore bathed in a broad stream of slowly flowing nitrogen gas in order to keep the surroundings free of unwanted moisture. Experiments in which the flow rate of the dry nitrogen was varied demonstrated that the droplet growth was unaffected at the flow rates that were utilized.

Most of the experiments were performed on borosilicate glass slides. They were immersed for 10 min in 10% HF solution and then washed repeatedly with distilled water. After drying, the slides were either directly used for the complete wetting experiments or silanized by immersing them in a solution of octadecyltrichlorosilane.<sup>3</sup>

The contact angle of water on the slides was investigated by direct measurement of the advancing and receding angles  $\theta_A$  and  $\theta_R$  of a sessile drop.<sup>4</sup> The drop was formed on the surface with a microliter syringe and an enlarged image of the drop was produced with a video camera. The contact angle could be measured directly on the screen and the advancing angle was observed when water was added to the drop from the syringe and the receding angle when water was withdrawn. The contact angles of the silanized slides were  $\theta_R = 110^\circ$  and  $\theta_A = 95^\circ$ , in good agreement with literature values<sup>4</sup> for similarly treated surfaces. The difference between the receding and advancing angles is a measure of the geometrical and chemical roughness of the surface.

The optical arrangement, which will be described

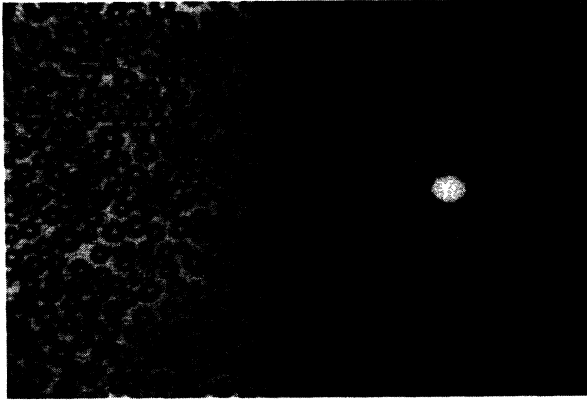


FIG. 1. Photograph of television screen showing simultaneous display of images in direct and transform space. The average size of the droplets is  $50 \mu\text{m}$ .

elsewhere,<sup>5</sup> was designed to study microscopic patterns with laser light, both by direct imaging of features  $1\text{--}300 \mu\text{m}$  in size and by small-angle light scattering in the range  $1500\text{--}15000 \text{cm}^{-1}$ . The images in both direct and transform space can be viewed on a television screen (Fig. 1) and recorded on video tape. The analysis was performed directly on the screen or by means of a computer after the images had been digitized.

In studies of surfaces that are wetted by the liquid,  $de/dt$ , the change in thickness  $e$  of the wetting layer with time, was determined from observations of the interference pattern of the film. Fringes are formed by the interference of the principal beam with the beam reflected by the slide-air interface and at the liquid-air interface. Although the contrast is low ( $1:10^3$ ), the fact that the fringes are moving much more rapidly than the surrounding pattern makes them sufficiently visible.

**Complete wetting.**—We have studied the variations of  $de/dt$  with  $t$ ,  $F$ , and  $\Delta T$ . The supersaturation is given by the difference in the saturation pressures at the two temperatures,  $\Delta p = p_G - p_S$ , which in the range of temperatures studied is proportional to  $\Delta T^{0.8}$ . Since temperature is the directly measured quantity we will generally express our results in terms of  $\Delta T$  rather than  $\Delta p$ . At constant  $\Delta T$  and  $F$ ,  $de/dt$  is independent of the time and the dependence on supersaturation (Fig. 2) and flow rate is consistent with the expression

$$de/dt = \alpha(w\Delta p/RT_S)(F/A)(M/\rho),$$

where  $R$  is the gas constant,  $M$  is the molar mass of the liquid,  $\rho$  is its density, and  $A$  is the cross-sectional area of the nozzle. The accommodation coefficient  $\alpha$  is approximately unity.

$\theta = 90^\circ$ .—When the surface is silanized, three different growth regimes are observed, depending on the

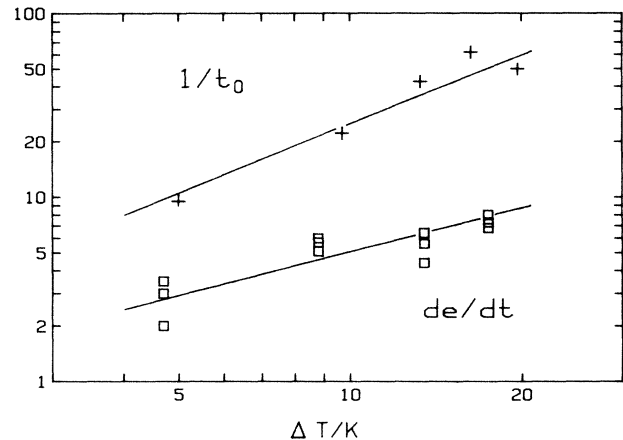


FIG. 2. Dependence of growth on the supersaturation. Squares:  $de/dt$ , rate of growth of the uniform layer in  $\mu\text{m s}^{-1}$  as a function of  $\Delta T$ . The slope of the line drawn through the points is 0.8, which corresponds to a unit slope in a plot vs  $\Delta p$ . Crosses:  $t_0^{-1}$  normalizing factor (in reciprocal seconds) required to superimpose measurements made at  $F = 5.2 \text{cm}^3 \text{s}^{-1}$  as a function of  $\Delta T$ . The line through the points has a slope of 1.3, which is equivalent to a slope of 1.6 in a plot vs  $\Delta p$ .

time. The characteristics of the droplet patterns in each regime can be described in terms of the droplet radii  $R$ , the polydispersity of the droplet size  $g = \Delta R / \langle R \rangle$ , the mean distance between droplets  $\langle a \rangle$ , and the surface coverage  $\epsilon^2 = (2\langle R \rangle / \langle a \rangle)^2$ .

At short times, typically  $t \leq 1 \text{s}$  after initiation of the flow, the surface is covered by a homogeneous pattern of small droplets with both  $R$  and  $a$  smaller than  $2 \mu\text{m}$ . The transmission of light through the liquid layer decreases and light is scattered at large angles. One can observe furious activity on the surface caused by coalescence of droplets.

The intermediate-time regime, typically  $1 < t \leq 300 \text{s}$  and  $2 < R \leq 300 \mu\text{m}$ , is characterized by the appearance of a well-defined order, as demonstrated by the structure factor, which exhibits a characteristic ring (Fig. 1). It can be shown from classical scattering theory<sup>6</sup> that the characteristics of the structure factor are determined by  $\langle R \rangle$ ,  $g$ , and  $\epsilon^2$ . In the intermediate regime the droplets grow at essentially constant polydispersity ( $g \approx 0.2$ ) and surface coverage  $\epsilon^2 \approx 0.5$ . Under these conditions there is a single peak in the structure factor whose position  $q_m$  corresponds to  $\langle a \rangle^{-1}$ . Thus, if one normalizes the scale by  $q_m$ , the droplet pattern remains remarkably constant with time.

Throughout this time period, there are two distinct mechanisms of droplet growth, as shown in Fig. 3, which shows the radius of an individual droplet as a function of the time. The growth of an isolated drop can be represented by the power law  $R \sim t^n$ , with  $n = 0.23 \pm 0.05$ . When neighboring droplets become

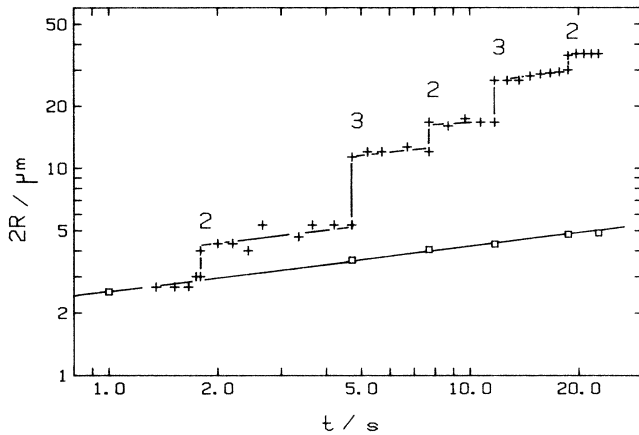


FIG. 3. Growth of a single drop. The numbers above the vertical segments indicate the number of droplets that have coalesced. The lower line of slope 0.23 has been obtained by displacing the segments between coalescences.

sufficiently large to touch, however, this growth is interrupted by coalescence. Two or more droplets merge very rapidly to produce a step change in the radius, but the power-law growth remains unchanged between these breaks.

The coalescence increases the rate of growth. This can be seen in the time dependence of  $q_m^{-1}$ , which, as a result of the constant surface coverage, is proportional to the time dependence of  $\langle R \rangle$ . We find  $q_m^{-1} \sim t^{n'}$  with  $n' = 0.75 \pm 0.05$ , as shown in Fig. 4, which shows data for runs made at a variety of flow rates and supersaturations.

Data from runs made at the same flow rate can be superimposed if they are displaced by a factor proportional to  $\Delta T^{1.3}$  (Fig. 2). A reasonably good normalization of all the runs can be obtained by shifting the data in proportion to  $F\Delta T^{1.3} \sim F\Delta p^{1.6}$ .

At very long times, typically  $t > 300$  s, small droplets form between the large droplets and the distribution of droplet sizes becomes bimodal. There is no obvious effect of the small droplets on the growth of the large ones and the pattern of growth remains unchanged until gravity causes the large droplets to become anisotropic and to begin to flow.

The mechanisms of condensation and growth must be different for the wetting and nonwetting cases; this is evident from the difference in the dependence on  $\Delta T$  and in the growth laws. If the droplets grew by the same mechanism as the film, i.e., directly from the vapor, the growth law would be

$$\begin{aligned} dV/dt &= 2\pi R^2 (dR/dt) \\ &= \alpha (w\Delta p/RT_S) (F/A) (M/\rho) \pi R^2. \end{aligned}$$

The first expression represents the volume increment of a drop, which according to this mechanism should

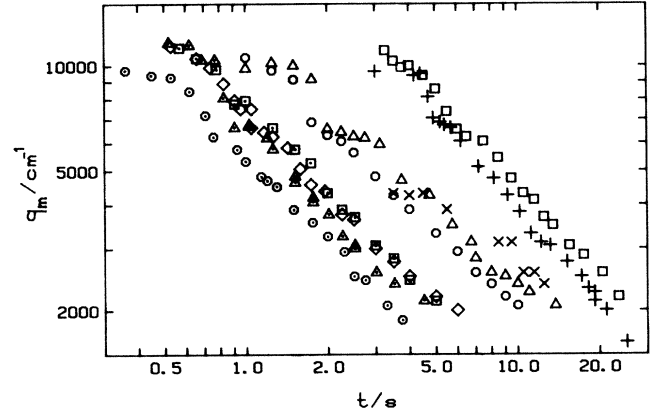


FIG. 4. Variation of  $q_m^{-1}$  with the time  $t$  for nine runs. Values of  $F$  in cubic centimeters per second and  $\Delta T$  in kelvins are respectively (pluses) 5.2, 5.0; (triangles) 12.4, 5.1; (circles) 5.2, 9.7; (squares) 2.1, 9.6; (crosses) 2.1, 13.5; (lozenges) 5.2, 13.3; (circles with center dot) 5.2, 16.3; (squares with center dot) 2.1, 16.3; (triangles with center dot) 5.2, 19.7.

be equal to the number of moles of substance per unit area per unit time that reach the droplet surface, the second expression. Thus, were this mechanism correct,  $\langle R \rangle$  would grow linearly with time and would depend on  $F\Delta p \sim F\Delta T^{0.8}$ ; the observed slow growth of droplets when  $\theta = 90^\circ$  and the stronger dependence on  $\Delta T$  are not predicted.

We propose instead a mechanism in which embryos of critical radius condense on the glass surface and diffuse to the growing droplets. The mechanism, which is roughly consistent with our results, has been shown to be applicable to the growth of solid islands by vapor condensation.<sup>7</sup> The surface of the glass slides is not uniform. This can be deduced from the observations that there is hysteresis in the contact angle and that droplets form at very low supersaturations. If the contact angle were  $\sim 90^\circ$  everywhere on the surface, nucleation theory<sup>7</sup> would predict that condensation would not occur until  $\Delta T \approx 25$  K. The nucleation rate  $J$  is a steep function of the contact angle and of the supersaturation:

$$J(\theta) \sim \exp[-A\sigma^3\phi(\theta)/\Delta p^2],$$

where  $\sigma$  is the surface tension of water,  $\phi = (2 - \cos\theta + 3\cos^3\theta)/4$ , and  $A$  is a constant. The observed nucleation rate is averaged over all sites by means of the distribution  $P(\theta)$ ,

$$\langle J \rangle \sim \int_0^\pi P(\theta) \exp[-A\sigma^3\phi(\theta)/\Delta p^2] d\theta.$$

At low supersaturations,  $\langle J \rangle$  is nonzero only for the smallest values of  $\theta$ , for which  $\phi \sim \theta^4$ , and we obtain  $\langle J \rangle \sim P(0)\Delta p^{1/2}$ .

The embryos will diffuse on the surface through a concentration gradient  $\nabla c$ , roughly determined by the distance between drops, which is of order  $R$ , and by the rate  $\langle J \rangle$ :  $\nabla c \sim \langle J \rangle / R$ . The surface diffusion constant  $D$  of the critical droplets can be taken as inversely proportional to the critical radius  $R^* \sim \Delta p^{-1}$ . Combining all of these factors leads to the growth equation

$$2\pi R^2 dR/dt \sim 2\pi R \nabla c \sim 2\pi F \Delta p^{3/2}$$

and the integrated expression  $R \sim [tF\Delta p^{3/2}]^{1/3}$ , which accounts reasonably well for the scaling we have found, but predicts a significantly stronger time dependence than is seen.

We have been unable to develop a description of the growth that includes coalescence. If, however, one assumes that the droplet pattern is self-similar throughout the intermediate time regime (an assumption in accord with the constancy of  $\epsilon$ ), it can be shown<sup>8</sup> that  $n' = 3n$ , a result in accord with our experiments.

We are particularly indebted to F. Perrot, who was involved with the early stages of the experiment, and

D. Fritter who assisted with the data analysis. We also acknowledge the contributions of H. Reiss and J.-L. Viovy to our understanding of the mechanism and the discussions with W. Goldberg and E. S. R. Gopal. This work was supported by the National Science Foundation.

---

(a)Permanent address: Service de Physique du Solide et de Résonance Magnétique, CEN-Saclay, 91191 Gif-sur-Yvette Cedex, France.

<sup>1</sup>T. J. Baker, *Philos. Mag.* **44**, 752 (1922); R. Merigoux, *Rev. Opt.* **9**, 281 (1937).

<sup>2</sup>P. G. de Gennes, *Rev. Mod. Phys.* **57**, 827 (1985).

<sup>3</sup>J. Sagiv, *J. Am. Chem. Soc.* **102**, 92 (1980).

<sup>4</sup>C. Allain, D. Auserre, and F. Rondelez, *J. Colloid Interface Sci.* **107**, 5 (1985).

<sup>5</sup>F. Perrot and D. Beysens, to be published.

<sup>6</sup>R. Hosemann and S. N. Bagchi, *Direct Analysis of Diffraction by Matter* (North-Holland, Amsterdam, 1962), p. 403.

<sup>7</sup>R. A. Sigsbee, in *Nucleation*, edited by A. C. Zettlemoyer (Marcel Dekker, New York, 1969).

<sup>8</sup>J.-L. Viovy, private communication.

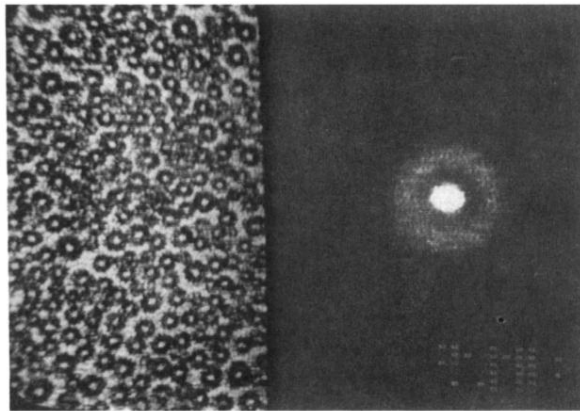


FIG. 1. Photograph of television screen showing simultaneous display of images in direct and transform space. The average size of the droplets is  $50 \mu\text{m}$ .